Molecular OR and AND logic gates: A theoretical proposal

M. Niţă and M. Ţolea

National Institute of Materials Physics, Atomistilor 405A, Magurele 077125, Romania

D. C. Marinescu ⬤

Department of Physics, Clemson University, Clemson, South Carolina 29634, USA

A conductance zero that results from the destructive quantum interference of the electron states in quantum transport between two given sites of a molecular system persists or disappears depending on the location of an externally applied perturbation. The *a priori* knowledge of the perturbation site that destroys or preserves a zero is the basis of an algorithm that outlines the creation of logic gates having external perturbations as inputs and a given conductance as output. Using a graph of the possible conductance paths between the various sites, we showcase the several different scenarios that correspond to AND/OR/XOR logical functions for a given set of contacts. This setup is shown to be independent of the strength of the coupling to the leads and magnitude of the perturbation. We illustrate this approach in the case of bipartite and nonbipartite single carbon cycle molecules (fulvene and benzene) and double carbon cycle molecules (naphthalene and biphenyl).

I. INTRODUCTION

Interference effects that occur in electron transport in quantum systems have been a generous source of theoretical and experimental investigations in the past 50 years or so. From the very beginning it was understood that the conductivity values can be affected by external parameters, such as the magnetic flux or disorder potentials, as present in the Aharonov-Bohm effect in mesoscopic rings and the associated conductance fluctuations [1,2]. The idea of manipulating the electron quantum state by the variation of some local external parameters is ubiquitous in molecular systems, i.e., chemical or quantum dot molecules. This lead to numerous applications such as transistors [3–5], thermoelectric and heat devices [6–8], and switching devices [9,10].

The predictable modification of the electron quantum state through the variation of external paramaters led also to the possible implementation of the Boolean functions, thus allowing the construction of logic gates with mesoscopic systems [11–13]. In this situation, the measurable output value is modified by the sequential or simultaneous application of two or more parameters, the logical inputs. For example, the six classical logic gates—two inputs/one output—can be created using a quantum system with a minimum of three points for which the input parameters are given by the matrix elements of the Hamiltonian, while the output is read from electron transmission or from the Heisenberg-Rabi oscillation frequency [14,15].

In this algorithm, the Hamiltonian matrix elements considered input parameters in evaluating transport properties are adjusted such that the desired logical function is obtained. This Hamiltonian based computing protocol leads to the experimental realization of molecular logic gates with the output given by the tunneling current through a scanning tunneling microscope tip or between externally connected electrodes.

As an example, the NOR logic gates were experimentally implemented with tri-naphthalene molecule in Ref. [16] or with long starphene in Ref. [17], the NAND logic gate with starphene molecule in Ref. [18], and the XOR logic gate with tetrabenzophenazine molecule in Ref. [19].

A different approach resulting in the construction of logic gates in quantum systems has been focused on the direct modification of the conditions that underlie the quantum interference of the electronic states. The propagation of quantum particles can be modified in several possible ways. The simplest example is a circular molecule or a quantum ring in which there are two possible trajectories between two points leading to an interference pattern of the electron wave functions whose maxima or minima correspond to associated values of the electric conductivity. External gates applied on one arm of a quantum ring can turn a destructive interference into a constructive one as in the OR logic gate proposed in Ref. [20]. Other gates were also designed in quantum rings [21–23], in circular molecules such as benzene [24–26] or multi-circular ones such as graphene [27], where the destructive or constructive interference conditions of the initial quantum state were determined by an external magnetic flux. External gates modified this status leading to the desired answer in the case of a specific logic gate.

In certain circumstances, however, conditions for the total destructive quantum interference (DQI) are created in the absence of any magnetic flux [28–30]. In this case, the conductivity cancellation is a result of different propagation paths in the energy space [31,32]. The presence of a DQI for the particle propagation between points i and j, is reflected macroscopically as a cancellation of the conductance $\mathbf{G}_{ij} = 0$ [30,33,34].

Previously [30,35], we formulated some general criteria that underlie the persistence of a zero in the presence of a perturbation selectively applied at certain lattice points. This

insight opens up a new direction in the realization of logic gates. Since for a given conductance zero it is *a priori* known where perturbations can be applied to maintain it or not, one can design logical functions whose input parameters are the strength of the perturbation, while the output is the value of the conductance. This idea is described in Sec. II of the paper where, after a short review of the previously obtained invariance properties, we show how logic OR/XOR and AND gates can be constructed using a visual representation for the nonzero conductance paths between the various sites. Sections III and IV illustrate the application of these considerations to the fulvene and benzene molecules, respectively, whose conductance zeros at several different propagation energies are theoretically derived in Ref. [28,30,35,36]. Moreover, we prove that this outcome does not depend on the strength of perturbation nor on the strength of the coupling with the leads. Section V is dedicated to exploring the posibility of creating logic gates by using two more complex molecules, such as naphthalene and biphenyl. The effective Hamiltonian method and the Green's functions that are used throughout the paper to calculate the logical outputs and transport properties are detailed in Sec. III A.

II. GENERAL DESCRIPTION OF THE METHOD

The system of interest is represented by a set of discretely localized quantum states $|i\rangle$ with $i \in \mathcal{M}$ connected through nonzero hopping elements. They can be the atomic orbitals as in the Hückel model of a molecule or quantum dot states as in an artificial molecule. The Hamiltonian,

$$H = \sum_{i,j \in \mathcal{M}} t_{ij} |i\rangle \langle j|, \qquad (1)$$

contains all the hopping matrix elements t_{ij} for $i, j \in \mathcal{M}$ written in terms of an energy unit t.

Throughout our paper, the hopping integral between nearest neighbors is taken as the energy unit (i.e., $t = 1$). Then, the connection to different physical systems with the same geometry can be done by adjusting the value of t. For the benzene molecule, for instance, the hopping energy has been calculated by density functional theory to be $t=2.6$ eV [24], similar values being used for other two-dimensional carbon structures [3,5,36]. For artificial molecular systems composed of quantum dots, the energy unit t can be tailored from the geometrical lengths. The Green's functions, calculated from H^{-1}, are expressed in $1/t$ units and the conductances in e^2/h units.

When a transport experiment is performed, two external leads are connected at sites i and j of the system and the $\mathbf{G}_{ij}$ conductance is calculated by the Landauer-Büttiker ansatz [33,37,38]. When the tunneling amplitudes of different paths in the position or energy space [29] cancel, a DQI is realized between sites i and j at energy E. Since the measured conductance between two points is proportional to the Green's function matrix element between the same points, $G_{ij} = [(E - H)^{-1}]_{ij}$ [30,33,34], we focus on the properties of the latter to develop our algorithm. To this end, we use the nonzero matrix elements of $(E - H)^{-1}$ as edges that connect vertices in the graph of the lattice sites to produce a visual map of the nonzero conductance paths. This is the inverse graph

representation of the non-DQI paths for a given system. For the energies considered in this problem, the matrix $(E - H)$ is nonsingular and its inverse exist. The shape of the inverse graph, however, changes as a function of the energy.

The persistence of a conductance zero $\mathbf{G}_{ij} = 0$ under the application of external perturbations depends on the location of the perturbation site, as discussed in Ref. [35]. A zero is preserved if the perturbation is applied at points that are nonadjacent vertices of i or j in the inverted graph. These points define the invariance set $\mathcal{M}_{\text{inv}}^i$:

$$\mathcal{M}_{\text{inv}}^i = \{k | G_{ik} = 0\}. \qquad (2)$$

Similarly, the invariance set associated with the lattice point j, $\mathcal{M}_{\text{inv}}^j$ contains all the points that are not connected with j in the inverted graph. Any multisite perturbation,

$$H' = H + \sum_{k,l \in \mathcal{M}_{\text{inv}}^{i,j}} w_{kl} |k\rangle \langle l| \qquad (3)$$

leaves the $i - j$ DQI process invariant. Any other invariance set derived by other methods, such as the interference point method in [30], will be a subset of $\mathcal{M}_{\text{inv}}^i$ or $\mathcal{M}_{\text{inv}}^j$.

The remaining sites define the sensitivity set which contains all the lattice points that have a Green's function connection with both i and j points, or a line in the inverted graph representation:

$$\mathcal{M}_{\text{sen}} = \{k | G_{ik} \neq 0, G_{jk} \neq 0\}. \qquad (4)$$

For a local perturbation of a quantum state $|s\rangle$ with s a sensitivity point from $\mathcal{M}_{\text{sen}}$,

$$H' = H + w_s |s\rangle \langle s|, \qquad (5)$$

the DQI process $G_{ij} = 0$ is destroyed and a nonzero value of conductance is obtained, $\mathbf{G}_{ij} \neq 0$ [35,39]. This behavior allows the construction of logic gates with the perturbation as input and the conductance value as output.

The on-site energies considered in this paper to generate a desired transport output are compatible with any experimental perturbation that can be applied to modify the local potentials, such as new external leads [3], Buttiker probes [5], heteroatom substitutions [6,39] and external gates [20,21,24,25]. In some experiments, the logical inputs were realized by interactions between the molecule with external Au and Al atoms [16–19]. Since all these situations lead to changes in the local (atomic) potentials therefore they are being incorporated in the present model as the single-site perturbations. Our formalism also applies to artificial molecules composed of connected quantum dots, since the local potential on each dot can be easily tuned experimentally.

Next, we present an algorithm for designing logic gates starting from the general properties of the inverted graph.

A. The AND gate

In designing an AND gate, we exploit the invariance property of a given zero $G_{ij} = 0$ under any perturbation Eq. (3). Here, we assume that the invariance sets $\mathcal{M}_{\text{inv}}^{i,j}$ are distinct,

$$\mathcal{M}_{\text{inv}}^i = \{j, x, \ldots\} \quad \text{and} \qquad (6)$$

$$\mathcal{M}_{\text{inv}}^j = \{i, y, \ldots\}, \qquad (7)$$

where $x \neq y$, i.e., $x \notin \mathcal{M}_{\text{inv}}^j$ and $y \notin \mathcal{M}_{\text{inv}}^i$.
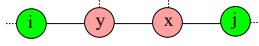
FIG. 1. The linear subgraph of the inverted graph for an AND logic gate. The three graph lines correspond to nonzero Green's functions G_{iy}, G_{yx}, and G_{xj}. The lines (i, j), (i, x) and (j, y) are missing which means $G_{ij} = 0$, $G_{ix} = 0$, and $G_{jy} = 0$. By applying two external perturbations on sites x and y the Green's function dependence $G'_{ij}(w_x, w_y)$ is an AND logical function.

In Fig. 1 we show the basic subgraph representing the distinct invariance sets for $G_{ij} = 0$. This is a linear graph containing three lines (i, y), (y, x) and (x, j) corresponding to three nonzero Green's functions G_{iy}, G_{yx} and G_{xj}, in agreement with Eqs. (6) and (7). For instance the invariance set $\mathcal{M}^i_{\mathrm{inv}}$ contains only the nonadjacent points of i, and they are x and j. Other points can be included, for as long they are different from y. From Eqs. (2), (6) and (7), $G_{ij} = 0$, $G_{ix} = 0$ and $G_{jy} = 0$ so the corresponding lines (i, j), (i, x) and (j, y) are missing from the inverted graph as shown in the figure.

If the above two distinct invariance sets exist one considers the following AND Hamiltonian:

$$H'_{\mathrm{AND}|\mathbf{G}_{ij}} = H + w_x|x\rangle\langle x| + w_y|y\rangle\langle y|, \tag{8}$$

with x, y two invariance points from the two distinct sets defined in Eqs. (6) and (7). By using two one-site parameters w_x and w_y as logical inputs one obtains an AND logical function for the conductance $\mathbf{G}_{ij}(w_x, w_y)$.

The proof follows from the Dyson expansion of the Green's function G'_{ij} of H'_{AND} which satisfies, up to the second order in perturbation,

$$G'_{ij}(w_x, w_y) \simeq G_{ij} + G_{ix}w_x G_{xj} + G_{iy}w_y G_{yj} + G_{iy}w_y G_{yx}w_x G_{xj}. \tag{9}$$

In this expression $G_{ij} = 0$, from the hypothesis, while $G_{ix}w_x G_{xj} = 0$ because $G_{ix} = 0$ from Eq. (6). Similarly, $G_{iy}w_y G_{yj} = 0$ because $G_{yj} = 0$ from Eq. (7). The second order term $G_{iy}w_y G_{yx}w_y G_{yj}$ is nonzero only when both w_x and w_y are non zero. This is the AND function behavior and, via the Landauer-Büttiker ansats [30], it is transferred to the conductance $\mathbf{G}_{ij}(w_x, w_y)$.

In summary, a logic AND gate can be realized if two distinct invariance sets of a DQI exist, i.e., for $G_{ij} = 0$, there are two different points x and y, each in a different invariance set, with the property $G_{xy} \neq 0$. The output of the gate is $\mathbf{G}_{ij}$ and the inputs are the perturbations applied at points x and y, w_x and w_y. This construct appears in the inverse graph $(E - H)^{-1}$ as a trilinear $i - y - x - j$ subgraph.

B. The OR gate

Realizing an OR logic gate hinges on the ability to identify two Hamiltonian parameters such that either one or both destroy a conductance zero. In this case, the sensitivity set of a given conductance zero $\mathbf{G}_{ij}$ has to contain at least two points,

$$\mathcal{M}_{\mathrm{sen}} = \{s, t, \ldots\}. \tag{10}$$

In the inverted graph representation, the common neighbors of sites i, j belong to the sensitivity set $\mathcal{M}_{\mathrm{sen}}$ [35], here the points designated by s, t. The square graph with no line
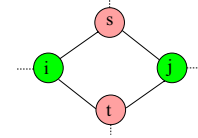

FIG. 2. A subgraph of the inverted graph that is useful to the design of the OR logic gate. A graph line (i, s) corresponds to a nonzero Green's function G_{is}, while the absence of an edge (i, j) means $G_{ij} = 0$. s and t are two common neighbors of i and j. The application of one or two external parameters w_s and w_t on the sites s and t leads to a non-zero Green's function $G'_{ij}(w_s, w_t)$, which establishes an OR logical function.

between i and j because $G_{ij} = 0$, relevant to the OR gate design is represented in Fig. 2. The edges are nonzero Green's function, while nonzero values of G_{is}, G_{js}, G_{it}, and G_{jt} are obtained, as the sites s and t are the common neighbors of i and j.

The OR perturbation Hamiltonian is,

$$H'_{\mathrm{OR}|\mathbf{G}_{ij}} = H + w_s|s\rangle\langle s| + w_t|t\rangle\langle t|, \tag{11}$$

with w_s, w_t the matrix elements of the local perturbations. The two on-site external parameters w_s and w_t are the OR logic gate inputs.

The Dyson expansion for the perturbed Green's function $G'_{ij}(w_s, w_t)$, is written as a first-order expansion in the perturbation as,

$$G'_{ij}(w_s, w_t) \simeq G_{ij} + G_{is}w_s G_{sj} + G_{it}w_t G_{tj}. \tag{12}$$

For $w_s = w_t = 0$ the function $G'_{ij}(0, 0) = G_{ij} = 0$.

For nonzero input parameters one obtains nonzero values of $G'_{is}(w_s, 0)$, $G'_{is}(0, w_t)$, $G'_{is}(w_s, w_t)$. The Green's function behavior is transferred to the conductance [28,30] and the conductance function $\mathbf{G}_{ij}(w_s, w_t)$ becomes an OR logical function. The particular values of w_s and w_t that give zero in the r.h.s. of Eq. (12) are omitted. Otherwise, if this were to happen, one obtains a XOR logical function.

In summary, an OR gate requires the existence of two points s and t outside the invariance sets, that is, the set $\mathcal{M}_{\mathrm{sen}}$ contains at least two points, where the applied perturbation modifies the G_{ij} zero. The OR (or under special conditions XOR gate) has as inputs the values of the perturbation applied at s and t, w_s and w_t, and as output G_{ij} or the corresponding conductance $\mathbf{G}_{ij}$. In the inverse graph representation, the corresponding subgraph is of a square or circular type $i - s - j - t - i$, which contains two double paths between i and j, $i - s - j$ and $i - t - j$, via s and t sites, respectively.

III. APPLICATIONS TO THE FULVENE MOLECULE AT $E = 0$

We illustrate the logic gates construction method in the case of a $N = 6$ fulvene molecule whose Hamiltonian H is depicted in Fig. 3(a).

The inverted graph of the fulvene molecule at $E = 0$ is presented in Fig. 3(b). The corresponding conductance zeros, represented by absent graph edges, as well as their invariance properties were derived in Ref. [30]. The non-zero Green's functions, associated with nonzero conductance values
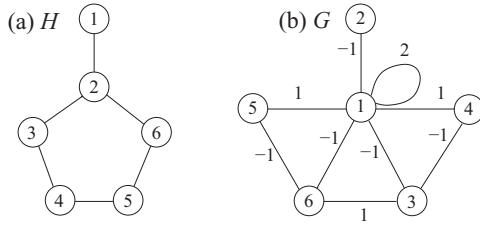
FIG. 3. The H graph of the fulvene molecule in (a). The inverted graph of fulvene and the values of the Green's functions are shown in (b). The missing lines in (b) indicate conductance zeros.

between the same points, are numerically calculated and their values are written on the corresponding graph edge.

A. The AND fulvene gate

To construct an AND gate we identify a conductance zero that has two different invariance sets. The relevant subgraph of this case, that was sketched in Fig. 1, involves points 4, 3, 6, and 5 of the inverted fulvene graph. This is shown in Fig. 4(a) where one notices the three-linear pattern 5-6-3-4. The Green function zero, $G_{45} = 0$, has two invariance sets, that contain the non-neighbor points 4 and 5, respectively: $\mathcal{M}_{\text{inv}}^{(4)} = \{2, 4, 5, 6\}$ and $\mathcal{M}_{\text{inv}}^{(5)} = \{2, 3, 4, 5\}$.

Below, sites 3 and 6 are selected for the perturbation applications, described by a Hamiltonian,

$$H'_{\text{AND}|G_{45}} = H + w_3|3\rangle\langle 3| + w_6|6\rangle\langle 6|, \quad (13)$$

where w_3 and w_6 are the input parameters of an AND logical function $G_{45}(w_3, w_6)$, even though the energies w_3 and w_6 do not modify $G_{45} = 0$ independently because $6 \in \mathcal{M}_{\text{inv}}^{(4)}$ while $3 \in \mathcal{M}_{\text{inv}}^{(5)}$. Two leads are attached to the fulvene lattice at the sites 4 and 5 as shown in Fig. 5. τ_l is the hopping energy on the leads. An incoming standing wave with wave number k and energy $E = 2\tau_l \cos k$ enters the system through L_2. The outgoing electron can be reflected into the lead L_2 or transmitted into L_1. Following Ref. [40], we calculate the conductance $\mathbf{G}_{45}$ of the connected molecule in the presence of the perturbation (13) for $E = 0$ ($k = \pi/2$). First, we use the effective Hamiltonian of the system in the presence of leads,

$$H_{\text{eff}} = H'_{\text{AND}} - i\tau|4\rangle\langle 4| - i\tau|5\rangle\langle 5|, \quad (14)$$

with $\tau = \tau_c^2/\tau_l$ where τ_c is the coupling constant between the leads and the sites 4 and 5 and τ_l the hopping energy on the leads [30,40].
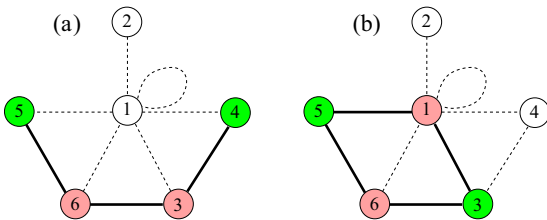

FIG. 4. The inverted graph of fulvene at $E = 0$. The relevant subgraphs for an AND function $\mathbf{G}_{45}(w_3, w_6)$ in (a) and for an OR function $\mathbf{G}_{35}(w_1, w_6)$ in (b) are drawn with solid lines.
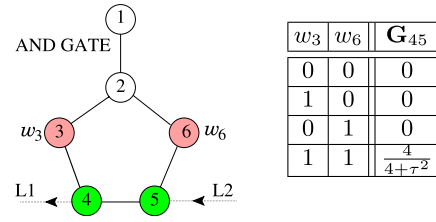

FIG. 5. An AND logic gate. $\mathbf{G}_{45}$ conductance in a fulvene device with two gates w_3, w_6 applied on the sites 3 and 6. The conductance is measured in e^2/h and the energy in the t units. τ measures the lead-molecule coupling strength.

The Landauer conductance is given by the formula:

$$\mathbf{G}_{45} = 4\frac{e^2}{h}\tau^2 |G_{45}^{\text{eff}}|^2, \quad (15)$$

where the effective Green's function G_{45}^{eff} satisfies a Dyson equation,

$$G_{45}^{\text{eff}} = G'_{45} - i\tau G'_{44}G_{45}^{\text{eff}} - i\tau G'_{45}G_{55}^{\text{eff}}. \quad (16)$$

G' is the Green's functions of Hamiltonian H'_{AND}. G_{55}^{eff} in turn satisfies,

$$G_{55}^{\text{eff}} = G'_{55} - i\tau G'_{54}G_{45}^{\text{eff}} - i\tau G'_{55}G_{55}^{\text{eff}}. \quad (17)$$

Finally, from Eqs. (16) and (17) we obtain

$$G_{45}^{\text{eff}} = \frac{G'_{45}}{1 + i\tau G'_{44} + i\tau G'_{55} + \tau^2 G'_{45}G'_{54} - \tau^2 G'_{44}G'_{55}}. \quad (18)$$

The Green's functions G'_{45}, G'_{55}, and G'_{44} involved in Eq. (18) are calculated from the Hamiltonian H'_{AND} in Eq. (13). Each satisfies a Dyson expansion. We start with G'_{45} and its involved functions:

$$G'_{45} = G_{45} + G_{43}w_3G'_{35} + G_{46}w_6G'_{65}, \quad (19)$$

$$G'_{35} = G_{35} + G_{33}w_3G'_{35} + G_{36}w_6G'_{65}, \quad (20)$$

$$G'_{65} = G_{65} + G_{63}w_3G'_{35} + G_{66}w_6G'_{65}. \quad (21)$$

The Eqs. (19), (20), (21) are simplified after introducing the cancellation of the Green's functions noted in Fig. 3(b): $G_{45} = 0$, $G_{46} = 0$, $G_{35} = 0$, $G_{33} = 0$ and $G_{66} = 0$. Solving for G'_{45},

$$G'_{45} = \frac{G_{43}w_3G_{36}w_6G_{65}}{1 - G_{36}w_6G_{63}w_3}. \quad (22)$$

For $G_{43} = -1$, $G_{36} = G_{63} = 1$ and $G_{65} = -1$ from Fig. 3(b),

$$G'_{45} = \frac{w_3w_6}{1 - w_3w_6}. \quad (23)$$

Similarly one obtains,

$$G'_{44} = \frac{w_3}{1 - w_3w_6}, \quad (24)$$

$$G'_{55} = \frac{w_6}{1 - w_3w_6}. \quad (25)$$

Introducing Eqs. (23), (24) and (25) in Eq. (18) one obtains:

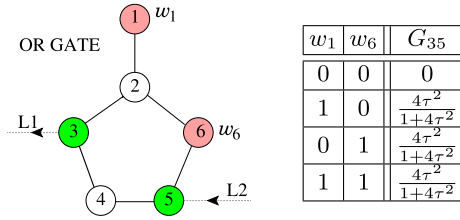$$G_{45}^{\text{eff}} = \frac{w_3w_6}{1 - w_3w_6(1 + \tau^2) + i\tau(w_3 + w_6)}. \quad (26)$$

FIG. 6. The logic OR gate in the fulvene lattice with two gates w_1, w_6. The Landauer conductance is evaluated at $E = 0$ in e^2/h units. τ measures the lead-molecule coupling.

With these, the conductance in Eq. (15) becomes,

$$\mathbf{G}_{45}(w_3, w_6)$$

$$= \frac{4\tau^2 w_3^2 w_6^2}{1 - 2w_3 w_6 + \tau^2\left(w_3^2 + w_6^2\right) + (1 + \tau^2)^2 w_3^2 w_6^2}, \quad (27)$$

an expression which corresponds to a logical AND function, since $\mathbf{G}_{45} \neq 0$ only when $w_3 w_6 \neq 0$. The conductance is measured in e^2/h.

A schematic representation of the AND logic gate, along with the numerical result is presented in Fig. 5. No other fulvene conductance zero can be used to build such an AND gate, since $\mathbf{G}_{45}$ is the only one that satisfies the conditions stated in Eqs. (6) and (7) and Fig. 1. In fact no other conductance zero has two distinct invariance sets as discussed in Ref. [30].

B. The OR fulvene gate

To build an OR gate we select a DQI process $G_{ij} = 0$ that has a sensitivity set with at least two different points. In Fig. 3(b) this corresponds to points i and j that have at least two common neighbors s and t. For instance, the sites 3-5, a DQI with $G_{35} = 0$, have two common neighbors 1 and 6, $\mathcal{M}_{\text{sen}} = \{1, 6\}$. This is represented by the square subgraph 1-3-6-5 in Fig. 4(b).

The OR Hamiltonian is therefore, in agreement with Eq. (11),

$$H'_{\text{OR}|\mathbf{G}_{35}} = H + w_1|1\rangle\langle 1| + w_6|6\rangle\langle 6|, \quad (28)$$

whose output is an OR logical function for the conductance $\mathbf{G}_{35}(w_1, w_6)$ when two transport leads are connected to the sites 3 and 5.

The molecule connected to leads is shown in Fig. 6 and the two perturbed sites 1 and 6 are marked.

Following the same calculation method as in Sec. III B one uses the effective Hamiltonian describing the contacted molecule,

$$H_{\text{eff}} = H'_{\text{OR}} - i\tau|3\rangle\langle 3| - i\tau|5\rangle\langle 5|, \quad (29)$$

which leads to an effective Green's function G_{35}^{eff} that determines the conductivity

$$\mathbf{G}_{35} = \frac{4\tau^2(w_1 + w_6)^2}{(1 - 2w_1 - w_1 w_6)^2 + 4\tau^2(w_1 + w_6)^2}. \quad (30)$$

This is an OR logical function with the input parameters w_1 and w_6. The input parameters of an OR gate are selected such that $\mathbf{G}_{35}(w_1, w_6) \neq 0$. If for instance one chooses $w_1 = -w_6$ in Eq. (30) an XOR gate is obtained.
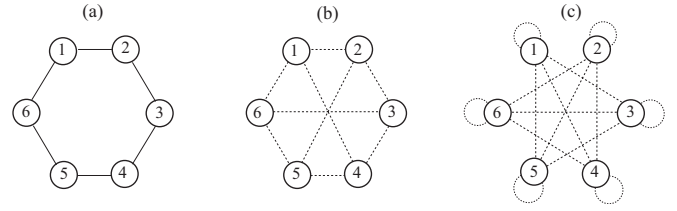

FIG. 7. The benzene molecule: (a) the graph of H; (b) the graph of $(H)^{-1}$; (c) the graph of $(\sqrt{2} - H)^{-1}$.

Particular results for different on-site w_1 and w_6 energies are given in the table from Fig. 6.

In contrast to the AND gate construction, there are many other options for the design of an OR function based on the fulvene quantum system. In the inverted graph in Fig. 3(b) there are other points i, j with $G_{ij} = 0$ and with at least two common neighbors for i and j. They correspond to the conductances $\mathbf{G}_{44}$, $\mathbf{G}_{46}$, $\mathbf{G}_{55}$, $\mathbf{G}_{35}$, $\mathbf{G}_{33}$, and $\mathbf{G}_{66}$. Their sensitivity sets contain at least two points and they can be used to design OR logic gates.

Other conductance zeros, such as $\mathbf{G}_{22}$, $\mathbf{G}_{23}$, $\mathbf{G}_{24}$, $\mathbf{G}_{25}$, $\mathbf{G}_{26}$, and $\mathbf{G}_{45}$ have only one common neighbor of their contact points and they can not be used to design an OR logic gate.

IV. APPLICATIONS TO THE BENZENE MOLECULE

The benzene molecule is represented in Fig. 7 by its Hamiltonian H in (a), while in (b) and (c) we show the inverse graphs, for $E = 0$ and $E = \sqrt{2}$, respectively, following calculations in Ref. [35].

A. Benzene logic gates at $E = 0$

The most well-known and studied example of DQI is the zero conductance in the benzene molecule with contacts in the meta position at $E = 0$ [3,28,36,41–45]. This corresponds, for example, to the Green's function $G_{13} = 0$ which will be used as a starting point in the following considerations.

1. No AND gate at $E = 0$

To investigate the possibility of an AND gate behavior of the 1-3 conductance we start from its related invariance properties. Following Ref. [35], G_{13} is invariant to multisite perturbations applied to nonadjacent points of site 1 which form $\mathcal{M}_{\text{inv}}^1 = \{1, 3, 5\}$, as shown in Fig. 7(b). For these points $G_{i1} = 0$. On the other hand, G_{13} is also invariant to the perturbations applied to the points not adjacent to site 3, $\mathcal{M}_{\text{inv}}^3 = \{1, 3, 5\}$. Since points 1 and 3 have identical sets of nonadjacent points, G_{13} has only one invariance set and a logic AND gate cannot be built at $E = 0$. This can be proven also by *reductio ad absurdum*. We assume that we found a logical AND function $G_{13}(w_x, w_y)$. This means that w_x taken alone does not modify G_{13}, indicating that x is an invariance point that belongs to $\mathcal{M}_{\text{inv}}$. The other disturbance w_y, taken separately, does not change G_{13}. So the point y also belongs to $\mathcal{M}_{\text{inv}}$. It results that $x, y \in \mathcal{M}_{\text{inv}}$ indicating that a multisite perturbation w_x, w_y does not change the zero. The hypothesis is contradicted.
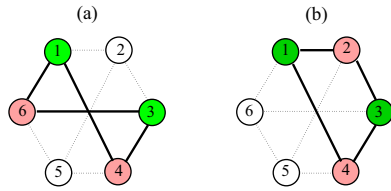
FIG. 8. The benzene inverted graph at $E = 0$. The OR subgraphs are drawn with solid lines. The logical functions involved are $G_{13}(w_4, w_6)$ in (a) and $G_{13}(w_2, w_4)$ in (b). The green points 1 and 3 exhibit a DQI with $G_{13} = 0$ for no external gates applied. The external gates leading to the logical function behavior of G_{13} are colored in pink.

2. OR/XOR gate

Benzene with meta contacts at $E = 0$ can be used to build logic gates of the OR (or XOR) type. To this end, we select points at which a perturbation changes a given zero $G_{13} = 0$. These are the points outside the invariance set, $\mathcal{M}_{\text{sen}} = \{2, 4, 6\}$, as shown in Fig. 7(b). These points that have a "Green's function link" with both contacts 1 and 3, indicating that all functions G_{i1} and G_{i3} with $i \in \mathcal{M}_{\text{sen}}$ are nonzero.

A unisite perturbation at sensitivity points as they are defined in Eq. (4) can modify an $i - j$ DQI process as shown in [35,39] and we use this property to build logic OR and XOR gates.

We consider points 4 and 6 from $\mathcal{M}_{\text{sen}}$, which separately modify G_{13}. w_4 modifies G_{13} and w_6 modifies G_{13}. Two cases arise: if they modify together G_{13} then $G_{13}(w_4, w_6)$ is the OR gate; and if not, we have the XOR gate.

To see for which values either the OR or the XOR gates is obtained, we calculate the effective Green's function G_{13}^{eff} for the effective Hamiltonian $H_{\text{eff}} = H'_{\text{OR}|\mathbf{G}_{13}} - i\tau|1\rangle\langle1| - i\tau|3\rangle\langle3|$ where the perturbed Hamiltonian is $H'_{\text{OR}|\mathbf{G}_{13}} = H + w_4|4\rangle\langle4| + w_6|6\rangle\langle6|$. The analytical calculation can still be done and we first obtain the effective Green's function:

$$G_{13}^{\text{eff}} = -\frac{w_4 + w_6}{4 + 2i\tau(w_4 + w_6)}. \qquad (31)$$

This gives us the conductance with the formula $\mathbf{G}_{13} = 4\tau^2 \frac{e^2}{h}|G_{13}^{\text{eff}}|^2$.

For $w_4 \neq -w_6$ in Eq. (31) we have the OR gate and we present the result for $w_4, w_6 = 0/1$ in Fig. 9. To emphasize that the obtained logical function is independent of the leads-molecule coupling the conductance is expressed in terms on the contact parameter τ.
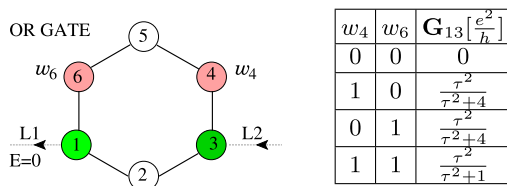

FIG. 9. The OR gate for benzene molecule at $E = 0$. The output of the logic gate is the meta conductance $\mathbf{G}_{13}$ and the inputs are the two external gates w_4 and w_6 applied on sites 4 and 6. The transport is calculated for the lead-molecule coupling $\tau = \tau_c^2/\tau_l$ and for wave number $k = \pi/2$.
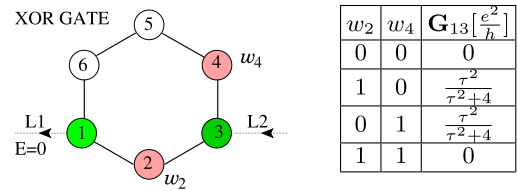

FIG. 10. The XOR gate for benzene molecule at $E = 0$. The output of the logic gate is the meta conductance $\mathbf{G}_{13}$ and the inputs are two external gates w_2 and w_4 applied on sites 2 and 4. τ is the lead-molecule coupling constant and wave number $k = \pi/2$.

A similar argument can be made for the creation of an OR gate using points 2 and 4 in the set $\mathcal{M}_{\text{sen}} = \{2, 4, 6\}$ to apply the logical inputs. The perturbed Hamiltonian becomes

$$H'_{\text{OR}|\mathbf{G}_{13}} = H + w_2|2\rangle\langle2| + w_4|4\rangle\langle4|, \qquad (32)$$

which gives OR/XOR logical function for G'_{13}. In the presence of contacts, when the Hamiltonian is transformed into $H^{\text{eff}} = H'_{\text{OR}|\mathbf{G}_{13}} - i\tau|1\rangle\langle1| - i\tau|3\rangle\langle3|$, the effective Green function between points 1 and 3 becomes

$$G_{13}^{\text{eff}} = \frac{w_4 - w_2}{(\tau w_4 - 2i)(\tau w_2 - 2i)}. \qquad (33)$$

This gives the conductance $\mathbf{G}_{13}$. This indicates that a logical OR function is obtained for any gates satisfying $w_2 \neq w_4$ and for any lead-sample coupling regime.

From Eq. (33), when the two external gates have equal energies $w_2 = w_4$, $G_{13}^{\text{eff}} = 0$, and the 1-3 DQI is restored. So for this particular case one obtains the XOR logical function. We present this case in Fig. 10 for inputs $w_2, w_4 = 0/1$ and output the 1-3 conductance.

We note that by moving the gate potential from the site 6 to site 2 in Figs. 9 and 10 the 1-3 constructive interference obtained for nonzero inputs is totally destroyed, G_{13} becomes zero, and the OR gate turns into an XOR one.

By using the inverted graph from Fig. 7(b), the two OR gates derived from the functions $G_{13}(w_4, w_6)$ and $G_{13}(w_2, w_4)$ can be identified starting from two circular/square subgraphs that are pictured in Figs. 8(a) and 8(b).

B. Benzene logic gates at $E = \sqrt{2}$

While previously we established that AND gates cannot be constructed in benzene at $E = 0$, here we explore the outcome of our algorithm for $E = \sqrt{2}$. In this case, the DQIs and zeros were calculated in Ref. [36], values we incorporate in the inverse graph $(\sqrt{2} - H)^{-1}$ from Fig. 7(c) which shows that only the lines between the ortho positions of benzene are missing. This is in agreement with the fact that $G_{12} = 0$. (All other zeros, $G_{23}, \ldots, G_{61}$ are of the same kind, i.e., ortho contacted benzene zeros).

The invariance sets of the ortho $G_{12} = 0$ are given by the nonadjacent points to 1 and 2, respectively [35]. From Fig. 7(c) we write the invariance set of point 1 as $\mathcal{M}_{\text{inv}}^1 = \{2, 6\}$, while the invariance set of point 2 is $\mathcal{M}_{\text{inv}}^2 = \{1, 3\}$. Thus, $\mathcal{M}_{\text{sen}} = \{4, 5\}$ is formed by the set of external points of the two invariance sets. We conclude therefore that an ortho zero can be used for OR gates because we have two points in
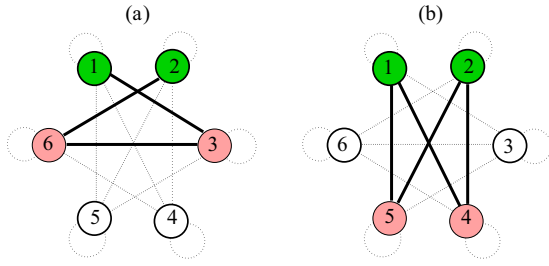
FIG. 11. The benzene inverted graph at $E = \sqrt{2}$. The AND/OR subgraphs are drawn with solid lines. The linear AND subgraph of the logical function $G_{12}(w_3, w_6)$ is shown in (a). The square subgraph for the OR logical function $G_{12}(w_4, w_5)$ is shown in (b). The green points 1 and 2 exhibit a DQI process at $E = \sqrt{2}$ having $G_{12}(\sqrt{2}) = 0$.

$\mathcal{M}_{\text{sen}}$, and it can also be used for an AND gate because it has two different invariance sets.

1. AND gate at $E = \sqrt{2}$

The fact that the ortho zero at $E = \sqrt{2}$ has 2 invariance sets means that it is possible to construct a logic AND gate starting from the known properties. To apply the general theory of the AND gate starting from $G_{12} = 0$, we identify two different points from the two invariance sets, $x \in \mathcal{M}_{\text{inv}}^1$ and $y \in \mathcal{M}_{\text{inv}}^2$, where $x \neq y$ with the additional property that $G_{xy} \neq 0$. These are points 3 and 6.

The input points of the logical function, 3 and 6, together with the contact points, 1 and 2, form a triple $1-2$ path, 1-3-6-2, as shown in Fig. 11(a). This is the only one trilinear subgraph that starts from 1 and ends at 2 as depicted in Fig. 1. That is, the only AND logical function with output $\mathbf{G}_{12}$ has two inputs, w_3 and w_6.

According to the general theory in Sec. II A, the dependence of the Green's function G_{12} on the input parameters w_3 and w_6 is a logic AND. An analytical formula for this function, is obtained by calculating the Green's function $G_{12}' = (\sqrt{2} - H')^{-1}$ of the perturbed Hamiltonian

$$H_{\text{AND}|\mathbf{G}_{12}}' = H + w_3|3\rangle\langle3| + w_6|6\rangle\langle6|. \tag{34}$$

From a Dyson equation we obtain,

$$G_{12}'(\sqrt{2}) = -\frac{w_3 w_6}{2 - \sqrt{2}w_6 - \sqrt{2}w_3 - w_3 w_6}, \tag{35}$$

which is obviously a logical AND function with input parameters w_3 and w_6.

Transferring the properties on the conductance $\mathbf{G}_{12}$ calculated at Fermi energy $E_F = \sqrt{2}$ we will obtain the AND gate function. The picture of the AND benzene device and a numerical result is shown in Fig. 12. The wave number involved in the transport calculation, from the formula $E_F = 2\tau_l \cos k$, is $k = \pi/4$, leads hopping energy is $\tau_l = 1$ and the lead-sample coupling $\tau = \tau_c^2/\tau_l = 1$.

2. OR gate at $E = \sqrt{2}$

Because $\mathcal{M}_{\text{sen}} = \{4, 5\}$, we consider $H_{\text{OR}|\mathbf{G}_{12}}' = H + w_5|5\rangle\langle5| + w_4|4\rangle\langle4|$ and show that the ortho component of the Green's function $G = (E - H')^{-1}$ is a logical OR function (or XOR in particular cases).
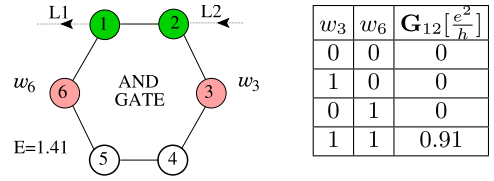

w_3	w_6	$\mathbf{G}_{12}[\frac{e^2}{h}]$
0	0	0
1	0	0
0	1	0
1	1	0.91

FIG. 12. The AND gate for benzene molecule at $E = \sqrt{2}$. The output of logic gate is the conductance $\mathbf{G}_{12}$ and the inputs are the two external gates w_3 and w_6 applied on sites 3 and 6. The transport is calculated for $\tau_c = 1$, $\tau_l = 1$, and $k = \pi/4$.

Analytically,

$$G_{12}' = \frac{w_4}{\sqrt{2} - w_4} + \frac{w_5}{\sqrt{2} - w_5}, \tag{36}$$

which behaves like an OR function for the values w_4, w_5 that give the nonzero numerator of the sum.

The OR gate device is sketched in Fig. 13 and the gate outputs are numerically calculated for the inputs values of w_4, w_5 equal to 0 and 1.

The subgraph related to OR logical function $G_{12}(w_4, w_5)$ is drawn on the inverted graph from Fig. 11(b). One notices that it contains two $(1, 2)$ paths, $1-4-2$ and $1-5-2$, via the sites 4 and 5, respectively. These suggest that the perturbation w_4, or w_5, respectively, can modify the 1-2 DQI process, in agreement with the OR logical function.

V. APPLICATIONS TO COMPLEX MOLECULES

In this section we extend our algorithm to molecules with more than one periodic structure. This process starts from the calculation of the inverse matrix of a given molecule and its graphic representation which is used to establish what logic gates can be built. Here we discuss the case of naphthalene and biphenyl at $E = 0$.

A. Naphthalene logic gates at $E = 0$

The naphthalene molecule, shown in Fig. 14(a), contains two hexagonal carbon cycles that share a common edge. The H^{-1} matrix and its nonzero elements are depicted as lines in the inverted graph in Fig. 14(b). This is a complete bipartite graph whose lines (i, j) have the property that i and j belong to two disjoined subsets $A = \{1, 3, 5, 7, 9\}$ and $B = \{2, 4, 6, 8, 10\}$.

A quantum device is constructed by connecting two external leads to the same subset of points $i, j \in A$, while two
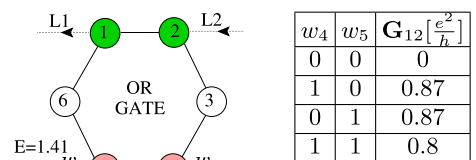

w_4	w_5	$\mathbf{G}_{12}[\frac{e^2}{h}]$
0	0	0
1	0	0.87
0	1	0.87
1	1	0.8

FIG. 13. The OR gate for benzene molecule at $E = \sqrt{2}$. The output of the logic gate is the conductance $\mathbf{G}_{12}$ and the inputs are the two external gates w_4 and w_5 applied on sites 4 and 5. The transport is calculated for $\tau_c = 1$, $\tau_l = 1$, and $k = \pi/4$.
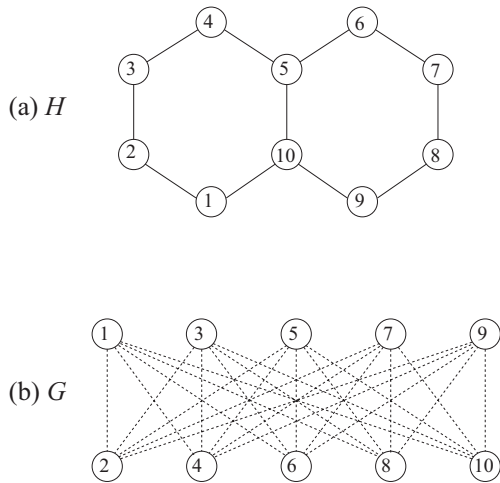
FIG. 14. The naphthalene molecule: the direct graph in (a) of H, and the inverted graph at $E = 0$ in (b).

external gates are applied on the two points $s, t \in B$. At $E = 0$, the electrical conductance

$$\mathbf{G}_{ij}(w_s, w_t) = \text{is an OR/XOR function.} \quad (37)$$

This is immediate due to the fact that the s, t points are common neighbors of the i and j points in the inverted graph and consequently the obtained subgraph is the one from Fig. 2. According to the result from Sec. II B, the Green function $G_{ij}(w_s, w_t)$ and the conductance in Eq. (37) are logical OR/XOR functions.

Our algorithm states that for any two contact points in the set $A = \{1, 3, 5, 7, 9\}$ one can construct an OR gate by choosing the inputs as two perturbations applied on B points. Figure 15 shows such an example when two transport leads are connected to points $i = 1$ and $j = 9$ and two external gates are applied on the sites $s = 4$ and $t = 6$. The effective function is calculated for the $H_{\text{eff}} = H'_{\text{OR}} - i\tau|1\rangle\langle1| - i\tau|9\rangle\langle9|$ with $H'_{\text{OR}} = H + w_4|4\rangle\langle4| + w_6|6\rangle\langle6|$. In the first order of approximations one obtains $G_{19}^{\text{eff}}(w_4, w_6) \simeq -\frac{2}{9}(w_4 + w_6)$ which is an OR logical function for input parameters w_4 and w_6. Beyond the perturbation limit, an exact numerical calculation of the $\mathbf{G}_{19}$ conductance is given in the Table of Fig. 15.

We remark that no AND function can be constructed with the naphthalene molecules at $E = 0$ as no trilinear subgraph—as the one in Fig. 1—can be found in its inverted graph.
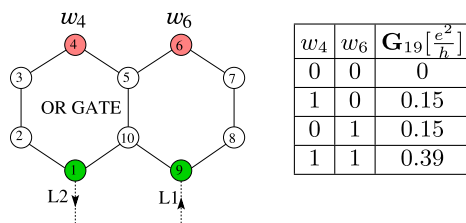

FIG. 15. The OR gate for naphthalene molecule at $E = 0$. The output of the logic gate is the conductance $\mathbf{G}_{19}$ and the inputs are the two external gates w_4 and w_6 applied on sites 4 and 6. The transport is calculated for $\tau_c = 1$, $\tau_l = 1$ and $k = \pi/2$.
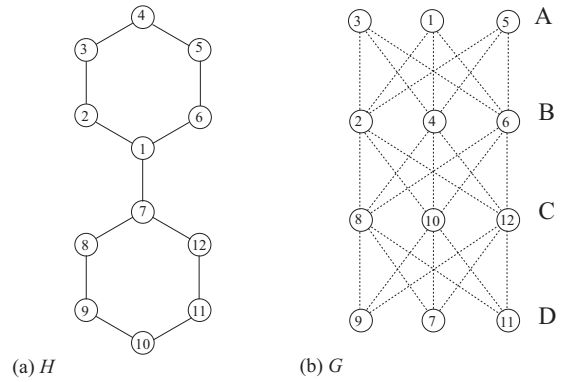

FIG. 16. The direct (a) and the inverted (b) graphs of the biphenyl molecule.

B. Biphenyl logic gates at $E = 0$

The biphenyl molecule is composed of two hexagon circles serial coupled as shown in Fig. 16(a). The graph lines (i, j) correspond to nonzero values of the Hamiltonian matrix elements H_{ij} with $i, j = 1, \ldots, 12$. The nonzero matrix elements of H^{-1} are represented as the graph lines (i, j) in Fig. 16(b).

From Fig. 16(b) one notices that the inverted graph is a 4-partite, this meaning that its points can be partitioned into 4 disjoint subsets, A, B, C, and D, with no line between the points in the same subset. The four subsets are marked on the Fig. 16(b).

In this case it is the possible to obtain an AND logic gate, as we show below. First, we note that every conductance

$$\mathbf{G}_{ij}(w_x, w_y) = \text{is an AND function,} \quad (38)$$

if the lead-molecule coupling points i, j are such that $i \in A$ and $j \in D$, and with perturbations w_x and w_y applied on the points $x \in B$ and $y \in C$.

The proof is immediate. Due to the 4-partite structure of the inverted graph from Fig. 16(b) the points i, j, x, y from Eq. (38) belong to a triple line subgraph i-x-y-j depicted in Fig. 1. Following Sec. II A, the conductance $\mathbf{G}_{ij}(w_x, w_y)$ is an AND function.

An AND logic gate with conductance as output can be obtained for biphenyl with lead-sample contact points $i = 3, 1, 5$ and $j = 9, 7, 11$. An example is given in Fig. 17 with $i = 1$ and $j = 9$. The effective function is calculated for the $H_{\text{eff}} = H'_{\text{AND}} - i\tau|3\rangle\langle3| - i\tau|9\rangle\langle9|$. The two perturbations are applied for the sites $x \in B$ and $y \in C$ from Fig. 16. One chooses $x = 2$ and $y = 8$ having $H'_{\text{AND}} = H + w_2|2\rangle\langle2| + w_8|8\rangle\langle8|$. In the first order of approximation one obtains $G_{39}^{\text{eff}}(w_2, w_8) \simeq \frac{w_2 w_8}{16}$ which is an AND function. The exact conductance is numerically calculated in the Table from Fig. 17 for input values 0 and 4 and, as expected, it exhibits the AND logical answer.

VI. CONCLUSIONS

In this paper we describe a general algorithm to create two types of logic gates-OR/XOR and AND-using as inputs external perturbations strategically applied on certain points of a quantum system and whose output is the conductivity between the other two points.
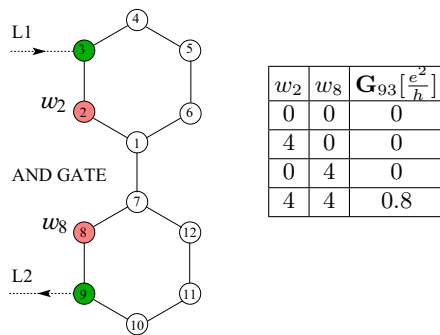
w_2	w_8	$\mathbf{G}_{93}\left[\frac{e^2}{h}\right]$
0	0	0
4	0	0
0	4	0
4	4	0.8

FIG. 17. The AND gate for biphenyl molecule at $E = 0$. The output of the logic gate is the conductance $\mathbf{G}_{93}$ and the two inputs are two external gates w_2 and w_8 applied on sites 2 and 8. The transport is calculated for $\tau_c = 1$, $\tau_l = 1$, and $k = \pi/2$.

Our approach uses the invariance of the electric conductance to multisite perturbations applied to a selected set of points called $\mathcal{M}_{\mathrm{inv}}$ [30,35]. When $\mathbf{G}_{ij} = 0$ has two distinct invariance sets we showed the algorithm to identify two points, one in each set, say x and y, such that the perturbations w_x and w_y acting on the two points are inputs to an AND gate.

The points in the sensitivity sets, $\mathcal{M}_{\mathrm{sen}}$ [35], represent sites where an applied perturbation modifies the $i - j$ DQI process. The perturbations w_s and w_t applied at s and t in $\mathcal{M}_{\mathrm{sen}}$ where used here to generate an OR/XOR gate.

This analysis was performed using the inverted graph method which enables a rapid identification of the four points - two input points and two for the output signal - involved in the logic gates design. This is done by looking at the relevant subgraph of a specific gate: a triple line for an AND gate and a square for an OR/XOR gate.

We applied these considerations to the particular cases of four different molecules, selected for their paradigm role: fulvene (one cycle, nonbipartite), benzene (one cycle, bipartite), naphthalene and biphenyl (two cycles). In each case we produced analytic results supporting our conclusions. Although an analytic derivation of the OR/XOR and AND gates can be done when the involved quantum system is small, our algorithm has the advantage that it can be applied to arbitrary larger structures for as long as the energy for which we calculate the conductance is not an eigenvalue of the Hamiltonian so that the inverted graph method is applicable.

[1] Y. Aharonov and D. Bohm, Significance of electromagnetic potentials in the quantum theory, Phys. Rev. **115**, 485 (1959).

[2] Y. Imry, *Introduction in Mesoscopic Physics* (Oxford University Press, Oxford, 2008).

[3] D. M. Cardamone, C. A. Stafford, and S. Mazumdar, Controlling quantum transport through a single molecule, Nano Lett. **6**, 2422 (2006).

[4] Y. Li, J. A. Mol, S. C. Benjamin, and G. A. D. Briggs, Interference-based molecular transistors, Sci. Rep. **6**, 33686 (2016).

[5] S. Chen, G. Chen, and M. A. Ratner, Designing principles of molecular quantum interference effect transistors, J. Phys. Chem. Lett. **9**, 2843 (2018).

[6] S. Sangtarash, H. Sadeghi, and C. J. Lambert, Connectivity-driven bi-thermoelectricity in heteroatom-substituted molecular junctions, Phys. Chem. Chem. Phys. **20**, 9630 (2018).

[7] R. Miao, H. Xu, M. Skripnik, L. Cui, K. Wang, K. G. L. Pedersen, M. Leijnse, F. Pauly, K. Wärnmark, E. Meyhofer, P. Reddy, and H. Linke, Influence of quantum interference on the thermoelectric properties of molecular junctions, Nano Lett. **18**, 5666 (2018).

[8] L. Ma, L.-L. Nian, and J.-T. Lü, Design and optimization of a heat engine based on a porphyrin single-molecule junction with graphene electrodes, Phys. Rev. B **101**, 045410 (2020).

[9] G. Ke, C. Duan, F. Huang, and X. Guo, Electrical and spin switches in single-molecule junctions, InfoMat **2**, 92 (2020).

[10] H. Zhang, M. Shiri, R. T. Ayinla, Z. Qiang, and K. Wang, Switching the conductance of a single molecule: Lessons from molecular junctions, MRS Commun. **12**, 495 (2022).

[11] R. Baer and D. Neuhauser, Anticoherence based molecular electronics: Xor-gate response, Chem. Phys. **281**, 353 (2002).

[12] S. Sangtarash, C. Huang, H. Sadeghi, G. Sorohhov, J. Hausser, T. Wandlowski, W. Hong, S. Decurtins, S.-X. Liu, and C. J. Lambert, Searching the hearts of graphene-like molecules for simplicity, sensitivity, and logic, J. Am. Chem. Soc. **137**, 11425 (2015).

[13] W.-H. Soe, P. de Mendoza, A. M. Echavarren, and C. Joachim, A single-molecule digital full adder, J. Phys. Chem. Lett. **12**, 8528 (2021).

[14] N. Renaud and C. Joachim, Classical boolean logic gates with quantum systems, J. Phys. A **44**, 155302 (2011).

[15] O. F. Namarvar, O. Giraud, B. Georgeot, and C. Joachim, Quantum Hamiltonian computing protocols for molecular electronics boolean logic gates, Quantum Sci. Technol. **4**, 035009 (2019).

[16] W.-H. Soe, C. Manzano, A. De Sarkar, F. Ample, N. Chandrasekhar, N. Renaud, P. Mendoza, A. Echavarren, M. Hliwa, and C. Joachim, Demonstration of a nor logic gate using a single molecule and two surface gold atoms to encode the logical input, Phys. Rev. B **83**, 155443 (2011).

[17] W. Soe, C. Manzano, P. de Mendoza, P. McGonigal, A. Echavarren, and C. Joachim, Long starphene single molecule nor Boolean logic gate, Surf. Sci. **678**, 163 (2018).

[18] D. Skidin, O. Faizy, J. Krüger, F. Eisenhut, A. Jancarik, K.-H. Nguyen, G. Cuniberti, A. Gourdon, F. Moresco, and C. Joachim, Unimolecular logic gate with classical input by single gold atoms, ACS Nano **12**, 1139 (2018).

[19] W.-H. Soe, C. Manzano, and C. Joachim, A tetrabenzophenazine low voltage single molecule xor quantum Hamiltonian logic gate, Chem. Phys. Lett. **748**, 137388 (2020).

[20] S. K. Maiti, Quantum transport in a mesoscopic ring: Evidence of an or gate, Solid State Commun. **149**, 1684 (2009).

[21] S. K. Maiti, Nand gate response in a mesoscopic ring: An exact result, Phys. Scr. **80**, 055704 (2009).

[22] E. Dehghan, D. S. Khoshnoud, and A. S. Naeimi, Nand/and/not logic gates response in series of mesoscopic quantum rings, Mod. Phys. Lett. B **33**, 1950431 (2019).

[23] D. Cricchio and E. Fiordilino, Quantum ring in a magnetic field: High harmonic generation and not logic gate, Adv. Theory Simul. **3**, 2000070 (2020).

[24] S. Mirzanian and A. Shokri, Electronic transport in a molecular junction as XOR and or gates, J. Phys. Chem. Solids **77**, 146 (2015).

[25] M. A. Abbas, F. H. Hanoon, and L. F. Al-Badry, Possibility designing XNOR and nand molecular logic gates by using single benzene ring, Solid State Commun. **263**, 42 (2017).

[26] A. Shokri, S. Safapour, and R. Sabbaghi-Nadooshan, Three-leg molecular transistors as molecular logic circuits: Design and modeling, Int. J. Mod. Phys. B **32**, 1850234 (2018).

[27] F. Khoeini, F. Khoeini, and A. Shokri, Peculiar transport properties in z-shaped graphene nanoribbons: A nanoscale NOR gate, Thin Solid Films **548**, 443 (2013).

[28] Y. Tsuji, E. Estrada, R. Movassagh, and R. Hoffmann, Quantum interference, graphs, walks, and polynomials, Chem. Rev. **118**, 4887 (2018).

[29] F. Evers, R. Korytár, S. Tewari, and J. M. van Ruitenbeek, Advances and challenges in single-molecule electron transport, Rev. Mod. Phys. **92**, 035001 (2020).

[30] M. Niţă, M. Ţolea, and D. C. Marinescu, Conductance zeros in complex molecules and lattices from the interference set method, Phys. Rev. B **103**, 125307 (2021).

[31] S. Gunasekaran, J. E. Greenwald, and L. Venkataraman, Visualizing quantum interference in molecular junctions, Nano Lett. **20**, 2843 (2020).

[32] H. Pan, Y. Wang, J. Li, S. Li, and S. Hou, Understanding quantum interference in molecular devices based on molecular conductance orbitals, J. Phys. Chem. C **126**, 17424 (2022).

[33] M. Büttiker, Four-terminal phase-coherent conductance, Phys. Rev. Lett. **57**, 1761 (1986).

[34] B. Ostahie, M. Niţă, and A. Aldea, Non-Hermitian approach of edge states and quantum transport in a magnetic field, Phys. Rev. B **94**, 195431 (2016).

[35] M. Niţă and D. C. Marinescu, Persistent destructive quantum interference in the inverted graph method, Phys. Rev. B **105**, 155303 (2022).

[36] P. Sam-ang and M. G. Reuter, Characterizing destructive quantum interference in electron transport, New J. Phys. **19**, 053002 (2017).

[37] R. Landauer, Spatial variation of currents and fields due to localized scatterers in metallic conduction, IBM J. Res. Dev. **1**, 223 (1957).

[38] Y. Imry and R. Landauer, Conductance viewed as transmission, Rev. Mod. Phys. **71**, S306 (1999).

[39] S. Sangtarash, H. Sadeghi, and C. J. Lambert, Exploring quantum interference in heteroatom-substituted graphene-like molecules, Nanoscale **8**, 13199 (2016).

[40] M. Ţolea, M. Niţă, and A. Aldea, Analyzing the measured phase in the multichannel Aharonov-Bohm interferometer, Physica E **42**, 2231 (2010).

[41] D. Nozaki and C. Toher, Is the antiresonance in meta-contacted benzene due to the destructive superposition of waves traveling two different routes around the benzene ring?, J. Phys. Chem. C **121**, 11739 (2017).

[42] R. Sýkora and T. Novotný, Comment on "Is the antiresonance in meta-contacted benzene due to the destructive superposition of waves traveling two different routes around the benzene ring", J. Phys. Chem. C **121**, 19538 (2017).

[43] P. Sautet and C. Joachim, Electronic interference produced by a benzene embedded in a polyacetylene chain, Chem. Phys. Lett. **153**, 511 (1988).

[44] D. Nozaki and C. Toher, Reply to Comment on "Is the antiresonance in meta-contacted benzene due to the destructive superposition of waves traveling two different routes around the benzene ring?", J. Phys. Chem. C **121**, 19540 (2017).

[45] R. Sýkora and T. Novotný, Graph-theoretical evaluation of the inelastic propensity rules for molecules with destructive quantum interference, J. Chem. Phys. **146**, 174114 (2017).